Journal of Non-Crystalline Solids 425 (2015) 183–189

Contents lists available at ScienceDirect

Journal of Non-Crystalline Solids

journal homepage: www.elsevier.com/ locate/ jnoncrysol

Siliceous mesocellular foams modified via a partitioned cooperative self-assembly process using hexane as pore swelling agent

Weijun Shan [a,b], Wei Wang [b,*], Hongqiang Ru [a,*]

[a] School of Materials and Metallurgy, Northeastern University, Shenyang, China
[b] Key Laboratory for Anisotropy and Texture of Materials of Ministry of Education, Northeastern University, Shenyang, China

ARTICLE INFO

Article history:
Received 10 April 2015
Received in revised form 27 May 2015
Accepted 6 June 2015
Available online 18 June 2015

Keywords:
Mesocellular foam;
Hexane;
Silica;
Bimodal mesopores

ABSTRACT

Siliceous mesocellular foams (S-MCFs), a series of mesoporous silicas with large and 3D-interconnected mesopores, have drawn great attention as a versatile support for various applications. In this work, we for the first time demonstrated that hexane can be an ideal pore swelling agent for the preparation of modified S-MCFs (designated as MS-MCFs) via a previously reported partitioned cooperative self-assembly (PCSA) process based on cheap silica precursor, i.e., sodium silicate (SS). The MCF structures can actually be achieved by simply adjusting the addition order of the hexane with respect to the first addition of SS under certain partitioning conditions. As a result, conventional MCF structures can be modified by either disordered (PCSA-I route, hexane being added before the 1st addition of SS) or ordered SBA-15 (PCSA-II route, hexane being added some interval time after the 1st addition of SS) mesophases, forming two series of bimodal mesopore systems, without resorting to additives or complicated synthetic process. The specific surface areas up to 600 $m^2 g^{-1}$, pore volumes up to 0.84 $cm^3 g^{-1}$, and bimodal pore sizes (1st series measuring 8–12 nm and the 2nd series of 12–24 nm) can be obtained. The control over interval time, in particular in the PCSA-II route, during which the condensation of the silicate species was allowed to proceed was found to be crucial for the evolution of bimodal pore system other than the normal MCF structures, i.e., the formation of MS-MCFs. The silicate synthesis strategy thus reported opens new pathways to the preparation and tuning of MCF structured silicas and will further promote their applications.

1. Introduction

In 1999, a new series of mesoporous silicas, called the mesocellular foams (designated as S-MCFs), was firstly prepared based on the self-assembly process through a $(S^0H^+)(X^-I^+)$ pathway and organic pore swelling strategy. Large spherical cell sizes up to 42 nm, large pore volumes and 3D interconnected pore system [1–3] have shown great potentials as efficient supports for enzymes/protein [4–6], drug molecules [7–9], CO_2 capturer [10–13] and catalysis [14–20], to name only a few. To further engineer the mesostructures of S-MCF silica is still imperative with an aim to suit and promote their various applications.

In the commonly used templating system, i.e., the P123/water system, the micellization of the triblock copolymers P123 is driven by the hydrophobic polyethyleneoxide (PPO) block with a hydrophilic EO corona [21]. The hydrophilic:hydrophobic volume ratio (V_H:V_L) of nonionic-surfactant-templating systems was suggested to account for the formation of mesophases with different curvatures and mesopore sizes, etc. [22]. With an increase in the amounts of pore swelling agent, the transition from cylindrical micelles to spherical micelles yields S-MCFs [23]. Addition of sufficient amount of pore swelling agents, e.g., trimethylbenzene (TMB), increases the hydrophobic volumes (V_L), and decreases the curvature of the mesopores, and therefore enlarges the mesopore sizes [1–3]. In our previous works, a partitioned cooperative self-assembly (PCSA) process was instead proposed to tune the V_H, which allows to manipulate the mesostructures in a facile and effective way [24,25]. Furthermore, it was also demonstrated that, instead of singly adjusting V_H, the manipulation of both V_H and V_L at the same time yielded interesting mesostructural features of the S-MCFs: more uniform cell size distributions and larger window sizes [26]. In particular, this PCSA process is based on sodium silicate rather than on TEOS, the latter of which is still the most often employed silica precursors, though the former is much cheaper.

Currently, the TMB is the predominantly used pore swelling agent [1–3,26], mainly due to its spherical symmetry and large solubility in the PPO cores and is chosen to tune the V_L effectively. In contrast, the hexane with linear hydrogencarbon chain shows less solubility in the PPO cores [27,28] and is thus rarely used as the pore swelling agent for the preparation of S-MCFs [29]. The pore swelling behavior of hexane in the synthesis of S-MCFs is still not fully researched. Very recently, Zhou and coworkers reported a four-component microemulsion-type

* Corresponding authors.
E-mail addresses: shanwj@lnu.edu.cn (W. Shan), wangw@atm.neu.edu.cn (W. Wang), ruhq@smm.neu.edu.cn (H. Ru).

http://dx.doi.org/10.1016/j.jnoncrysol.2015.06.007
0022-3093/

system (P123/n-butanol/TMB/H_2O system) to prepare the S-MCFs with bimodal mesostructures [30,31] and further demonstrated their superior hydrodesulfurization performance over their monomodal mesoporous silica counterparts [31].

Herein, using the hexane as pore swelling agent, this work aims to unveil its roles in inducing/shaping the S-MCF structures. The synthetic procedure is based on the cheap sodium silicate, while the PCSA process further enables the facile and flexible tuning of resultant S-MCF structures without resorting to complex templating system or additional inorganic/organic additives. Two series of S-MCFs with modified S-MCF structures (designated as MS-MCFs) can therefore be obtained without using any additives or complicated synthetic process. It is believed that this work might open a new way to tuning the mesostructures of S-MCFs and especially the MS-MCFs, and might promote their versatile application in various fields.

2. Materials and methods

2.1. Chemicals

Sodium silicate ($Na_2SiO_3 \cdot 9H_2O$, Na_2O:SiO_2 molar ratio of 1.03 ± 0.03), n-hexane and c-HCl (37%) were purchased from the Sinopharm Chemical Reagent Co., Ltd. Pluronic PEO_{20}–PPO_{70}–PEO_{20} (P123 with M_w ~5800) was purchased from Aldrich. All the chemicals were used as received.

2.2. Conventional synthesis of S-MCFs from SS using hexane as pore swelling agent

The S-MCFs were synthesized via conventional methods with differing amounts of hexane. Typically, the clear P123 solution was prepared by dissolving 4.0 g P123 in 120.0 g deionized (DI) water and 20 mL c-HCl at 40 °C under stirring, to which various amounts of hexane were added. After mixing for 1 h, a solution of 10.5 g sodium silicate (SS) dissolved in 10.5 g DI water was then added dropwise. The mixture was stirred for another 6 h at 40 °C and then aged at 95 °C for another 20 h statically. After collection by filtration, washing and drying, the as-prepared samples were calcined at 550 °C for 4 h with a heating ramp of 1.5 °C min^{-1}. The samples were denoted as X*n*SS10.5, where the 'X*n*' stands for the amounts of hexane added (n = 2.0, 4.0, 7.0 g), and 'SS' denotes the sodium silicate precursor; '10.5' is the mass of SS.

2.3. PCSA-I route

All the synthetic details are the same as those in the conventional procedure shown above except the partitioned addition of SS: after 1 h stirring of the mixture of hexane/P123/HCl (aq.), a solution of 1st part SS 5.0 g dissolved in 5.0 g DI water was dropped slowly into the above mixture, with the 2nd part SS 5.5 g dissolved in 5.5 g DI water being added after some interval time. The final calcined samples were designated as X*n*SS5-*t*-5.5, where '*t*' denotes for the interval time (t = 0.5–3 h).

2.4. PCSA-II route

In this work, the hexane was also added with some interval time after the 1st addition of SS but before the 2nd. Typically, to the mixed solution of P123 and HCl, a solution of 1st part SS 5.0 g dissolved in 5.0 g DI water was dropped into the above mixture. After some interval time, the hexane was added and stirred for 5 min. The 2nd part SS 5.5 g dissolved in 5.5 g DI water was finally added. All the rest of the steps are the same as those for the PCSA-I route described above. The obtained samples were denoted as SS5-*t*X*n*-5.5, with the same definitions of the letters as shown above.

2.5. Characterization

Powder XRD patterns at 2θ angles from 0.6° to 3° were recorded at an interval of 0.02° (angular deviation of 0.0001°) on a Bruker D8 Advance diffractometer using Cu Kr radiation (40 kV, 120 mA). Transmission electron microscopy was performed using a FEI Tecnai *G2* F20 instrument operated at 200 kV. Nitrogen adsorption–desorption isotherms were measured at −196 °C using Tristar 3020 volumetric adsorption analyzers manufactured by Micromeritics (Norcross, GA). Before adsorption measurements, the samples were out-gassed under vacuum for at least 2 h at 200 °C. The specific surface areas of the samples were calculated using the BET method within the relative pressure range of 0.04 to 0.2. The pore size distributions were determined using the BJH method [32] with the film thickness (t) calibrated for spherical pores according to the BDB method [33–35]. The mesopore size distributions (PSDs) of the cell sizes and window sizes were calculated on the basis of adsorption and desorption branches of nitrogen isotherms, respectively. The total pore volume was estimated from the amount adsorbed at a relative pressure (P/P_0) of about 0.996.

3. Results and discussion

In this work, hexane was selected as the pore swelling agent to modify the mesoporous cellular silicas via the previously reported partitioned cooperative self-assembly process using SS as precursor [25,26], and as a control, the S-MCFs were also prepared via the conventional process. In the PCSA process without using pore swelling agent, the total amounts of SS were divided into two parts (1st addition and 2nd addition), with the 2nd part SS being added with some interval time after the 1st part. In order to magnify the partitioning effect, the 1st and 2nd additions of SS were all fixed to be 5 and 5.5 g (in the form of 50 wt.% SS aqueous solution) [25]. Via the PCSA process, the silicate/PEO interface structures formed by the initial deposition/penetration of silicate species into the PEO coronas of P123 micelles can be facilely controlled by tuning the interval time, because the rapid condensation reaction between silicate species and the self-assembly process with P123 can be delayed in a controllable way. Therefore, the V_H and thus the V_H/V_L can be controlled. The change of the V_H/V_L and its direct influence on curvatures of the silicate/P123 interface and eventually the mesostructures, including the mesopore sizes and microporosity, can be tailored [25]. In the preparation of MS-MCFs, the additions of the hexane with respect to the 1st addition of the 1st part SS are also keys to tuning the MS-MCF structures, because the tuning of V_H is now overlapped with the swelling process of hexane in the hydrophobic cores. Importantly, the silicate/P123 interface also has a great influence on the swelling behaviors of hexane in PPO cores of P123 micelles. In this work, according to the way the hexane was added to the synthesis mixture with respect to the addition of SS, two routes were proposed: one is called the PCSA-I route (XnSS5-*t*-5.5), where hexane was added 1 h before the first addition of SS; the other is called the PCSA-II route (SS5-*t*Xn-5.5), where the hexane was added shortly (5 min) before the second addition of SS. More details can be found in the Materials and methods section. The manipulation of the MCF structure and especially the MS-MCF structures is the main target of this work.

3.1. MS-MCFs via the PCSA-I route

In the PCSA-I route, the hexane was added conventionally, some time preceding the first addition of silica precursor (SS). In order to further investigate the mesopore structures obtained, the N_2 sorption measurements were conducted, with the results shown in Fig. 1. It can be seen from Fig. 1a that, for both PCSA-I and conventional route derived samples, the isotherms all show to be type IV isotherms with H2 hysteresis loops. The relative shallow N_2 capillary condensation steps at high P/P_0 between 0.7 and 0.9 were accompanied by rather

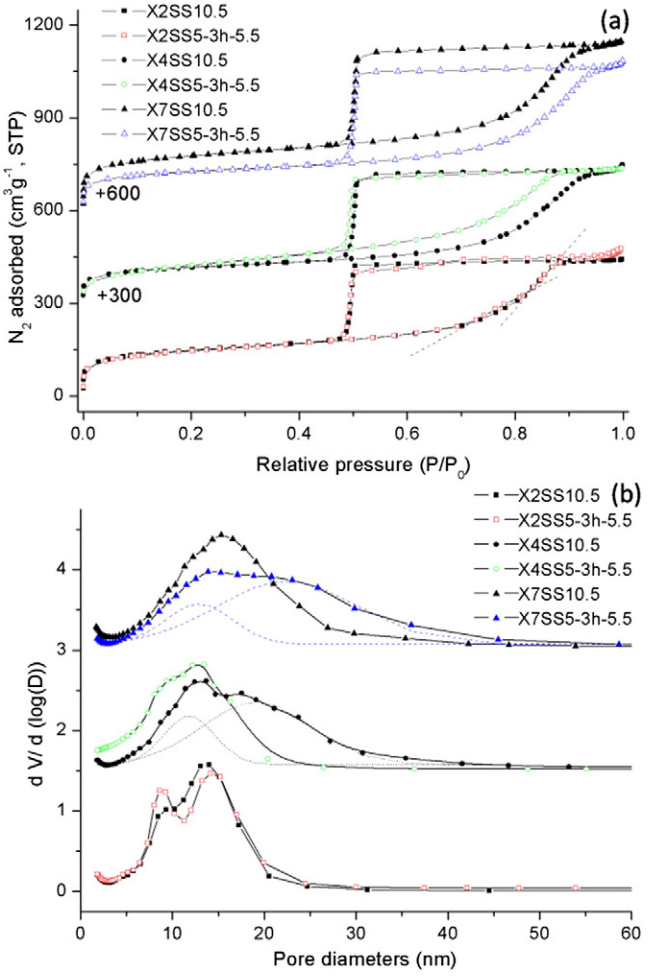

Fig. 1. N_2 isotherms (a) and pore size distributions (b) of S-MCFs prepared via conventional method and PCSA-I route using hexane as pore swelling agent and SS as silica precursor. In (a), some isotherms were shifted upward for clarity. The dashed lines were drawn to show the two steps in the capillary step, choosing X2SS5-3h-5.5 as representative. In (b), some pore size distribution curves were de-convoluted using Gaussian fitting to aid the discrimination of multiple pore size distributions.

sharp desorption steps taking place at much lower relative pressures (P/P_0 ~0.5). These results show that the formed mesostructures are composed of large cell pores with broadened cell pore size distributions, and the window pores that connect the cell pores are much smaller than the cell pores [36,37], causing significant delay in the capillary evaporation process. Such kinds of mesoporous silicas resemble those S-MCFs previously prepared via the conventional method using the TMB as pore swelling agent [26], suggesting the templating of the silicate species by spherical P123 micelles.

Additionally, according to the cell size distributions of mesoporous silicas shown in Fig. 1b, the cell sizes only increase from 10 nm to around 20 nm with the increase in the hexane dosages (Fig. 1b and Table 1), indicating the limited swelling of the P123 micelles with the increased hexane. In contrast, the same amounts (in mass) of TMB can increase the cell size up to 50 nm, although the window sizes are in the same level [26]. This means that the solubility of the pore swelling agents in the P123 dictates the micellar sizes and consequently the cell sizes. Compared with the TMB, the hexane is not effective in producing MCFs with large cell sizes, neither the large window sizes.

By further examining the cell size distributions shown in Fig. 1b, there is an interesting phenomenon observable, that is the appearance of the bimodal cell size distributions in these S-MCFs prepared using hexane as pore swelling agent. In some of these S-MCFs prepared via both the conventional method and the PCSA-I route, a series of

Table 1
Physicochemical properties of prepared S-MCFs.

Samples	BET/$m^2 \cdot g^{-1}$	V_{total}[a]/$cm^3 \cdot g^{-1}$	D_{cell}[b]/nm	D_{window}[c]/nm
X2CS10.5	500	0.69	9.4/13.6	<4
X4CS10.5	392	0.67	11.8/19.3	<4
X7CS10.5	598	0.85	15.6	<4
X2SS5-3h-5.5	494	0.74	8.8/14.3	<4
X4SS5-3h-5.5	434	0.67	9.1/12.9	<4
X7SS5-3h-5.5	424	0.75	12.7/22.7	<4
SS5-1hX2-5.5	470	0.63	10.0/19.2	<4
SS5-1hX4-5.5	454	0.67	10.4/w	<4/7.1
SS5-1hX7-5.5	529	0.72	12.4/16.4	<4/7.6
SS5-3hX2-5.5	484	0.67	8.4/w	<4/6.7
SS5-3hX4-5.5	595	0.84	8.5/w	<4/6.9
SS5-3hX7-5.5	588	0.83	8.7/11.9	<4/6.9

[a] Total pore volume based on the N_2 adsorbed at P/P_0 ~0.996.
[b] Cell size calculated on the adsorption branches according to the BDB method, the maximum on the PSDs.
[c] Window sizes calculated on the desorption branches according to the BDB method. In these S-MCFs, the window PSDs did not show a maximum, indicative of a smaller window size than 4 nm.

relatively small cell pores (10 ± 2 nm) can be observed, consistent with the pore size of monomodal S-MCF reported by Zhang and coworker based on hexane as pore swelling agent [29]. Such mesopore sizes are actually consistent with those of conventional SBA-15 prepared in the absence of pore swelling agent [25,38,39], suggesting the limited swelling of hexane in some P123 micelles. It should be pointed out that such mesopores, though a bit small in sizes, should still be spherical and therefore should be called to be MCFs too, because cylindrical mesopores of 10 ± 2 nm will produce capillary evaporation at higher P/P_0 of 0.6 or higher in the desorption branches [25,38,39].

This is different from those of S-MCFs prepared from TMB as pore swelling agent and the SS as precursor, where monomodal cell size distributions were always observed [26]. So, the formation of MS-MCFs cannot be perfectly explained by the known microemulsion droplets templating mechanism, which involves the rather uniform swelling of the P123 micelles by TMB molecules and thus the formation of uniform S-MCF structures [1–3], as supported by the correlated microemulsion droplet sizes and final MCF cell sizes [3]. Apparently, the only difference lies in the pore swelling agent employed. In this work, it is proposed that there are different forms of micelles in hexane/P123/HCl (diluted) system under the synthetic conditions employed, including the hexane-rich phases due to macroscopic phase separation [29]. The formation of mesostructures with small mesopores (10 ± 2 nm) can therefore be attributed to the presence of P123 micelles with limited solubilized hexane with linear hydrocarbon chains [27], while the second mode of cells with large sizes arise from the templating of swollen P123 micelles by hexane.

Furthermore, it should be pointed out that the PCSA-I route favors the formation of bimodal MS-MCFs compared with the conventional method, especially in view of preserving the 1st mode cell pores with smaller sizes (10 ± 2 nm). As shown in Fig. 1b, with high amount of hexane (e.g., X7 series), the X7SS10.5 shows to be monomodal, while X7SS5-3h-5.5 still shows to contain bimodal pores. This should thank the partitioned addition of SS to the synthesis mixture. In the conventional synthesis, the total SS was added at a time, and wide-spread hydrolysis and condensation reaction will consolidate the silicate/PEO interface rapidly. Such silicate covered P123 micelles, with more or less hexane, will follow a cooperative self-assembly process to form large aggregates and then precipitate out. In contrast with the conventional process, there are limited amounts of SS and therefore the silicate species in the PCSA-I route before the addition of the second part SS, so the condensation reaction promoted self-assembly process is to a great extent suppressed [25,26]. It has been reported that the corona thickness is negligibly influenced by the solubilized hexane [27]. In such less swollen micelles (thus smaller micellar sizes) and therefore high curvatures silicate/P123 micelles will result and the PEO chains will

become closer in distance. The condensation reactions between silicates penetrated into PEO coronas will be favored. The interface of these silicate/P123 hybrid mesostructures is expected to be more rigidified and therefore less interfered by the presence of hexane. Such silicate/P123 hybrid mesostructures will be consolidated upon the addition of the second part SS. In order to attest this proposition, a series of S-MCFs, as control, were prepared with short interval times. With much shorter interval time (e.g., 1 h or less), the condensation reaction between silicate coated P123 micelles will result in less rigidified silicate/P123 interfaces than those in the synthesis of X7SS5-3h-5.5, the preferential consolidation effect of the smaller P123 micelles might not be as prominent as in the case of X7SS5-3h-5.5, and monomodal S-MCFs might result. This deduction was attested by the N_2 sorption results shown in Fig. 2, where both X7SS5-0.5h-5.5 and X7SS5-1h-5.5 produce only monomodal MCF structures. This means that the control of condensation reactions of inorganic species by the PCSA-I route does play a crucial role in the synthesis of MS-MCFs.

In order to further examine the bimodal mesostructures of obtained MS-MCFs, especially the distributions of two mode cells/pores, TEM measurements were carried out, with results shown in Fig. 3 (more can be found in Fig. S1, Supplementary data). Clearly, two mode mesopores can surely be observed: one series of small mesopores (1st mode) is around 8 nm, the other is the typical MCF structures with large mesopores. Especially, the 1st mode mesopores tend to form small separate areas, resulting in a mixed mesophases in an individual particle. This is in good consistency with prior discussion on the N_2 sorption results on PCSA-I route derived MS-MCFs, namely the preferential condensation/consolidation of the silicate species coated on spherical P123 with higher curvatures (and therefore smaller pores). Therefore, via the PCSA-I route, the M-MCF silica is actually a mixed mesophase, where normal MCF structure is modified by a series of disordered small mesopores, forming a bimodal mesopore system.

3.2. PCSA-II route for MS-MCFs

In previous work dealing with the preparation of S-MCFs using TMB as pore swelling agent, we have demonstrated that simply altering the addition order of the TMB can yield an interesting series of unconventional S-MCFs, where small ordered SBA-15 regions were embedded in the disordered MCF matrix [26]. In this work, hexane was used as the pore swelling agent, then whether or not can similar measures lead to unusual MCFs? Therefore, a similar adjustment to the order of the hexane was made with respect to the 1st addition of SS. This

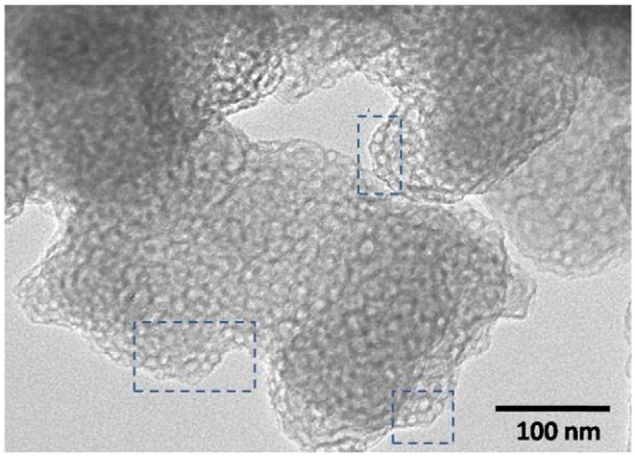

Fig. 3. Representative TEM image of the X2SS5-3h-5.5.

procedure was designated as the PCSA-II route, where hexane was added with some interval time after the 1st part SS.

The N_2 sorption results were shown in Figs. 4 and 6 and Table 1. The obtained isotherms and the PSDs derived from the adsorption branches show some interesting features:

(1) For the MS-MCFs prepared with short interval time, e.g., 1 h, the isotherms of MS-MCFs with different amounts of hexane are similar to those shown in Fig. 1, except that the mesopores with sizes of around 10 nm get much more prominent compared with those prepared via the PCSA-I route. The pore size distributions for large mesopores on the other hand become greatly broadened, showing a significant tailing in the PSDs presented as the inset in Fig. 4. This can be attributed to the low solubility of hexane in the P123 and inhomogeneous swelling of hexane in the silicate coated P123 micelles. Moreover, in the desorption branch, notable desorption steps at P/P_0 of 0.5–0.7 indicate that the first mode of mesopores (~10 nm) has shown to be different from those reported in Fig. 1. The 1st mode mesopores are more of cylindrical rather than spherical ones, as shown in the case of PCSA-I. According to the low-angle XRD pattern shown in Fig. 5 (curve d & e), the first modal mesopores still show a lack of long-range ordering, evidenced by much less resolved (100) peaks and the missing of XRD reflections at high angles. This

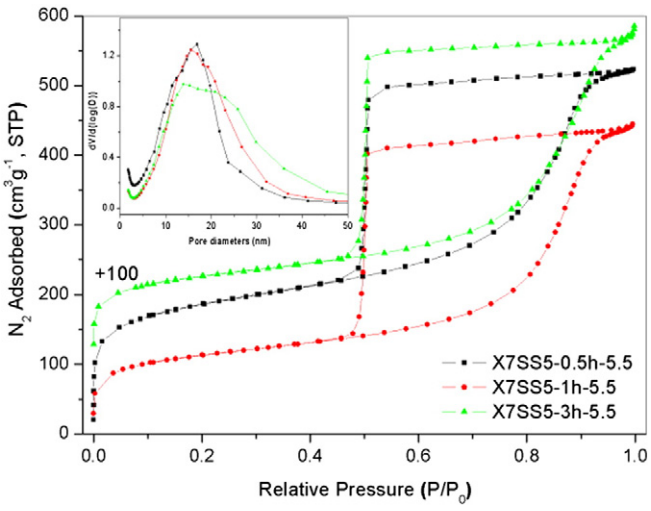

Fig. 2. N_2 sorption results of PCSA-I derived MS-MCFs with varying interval times but fixed addition combinations. The inset (left) shows the corresponding PSDs calculated on the adsorption branches.

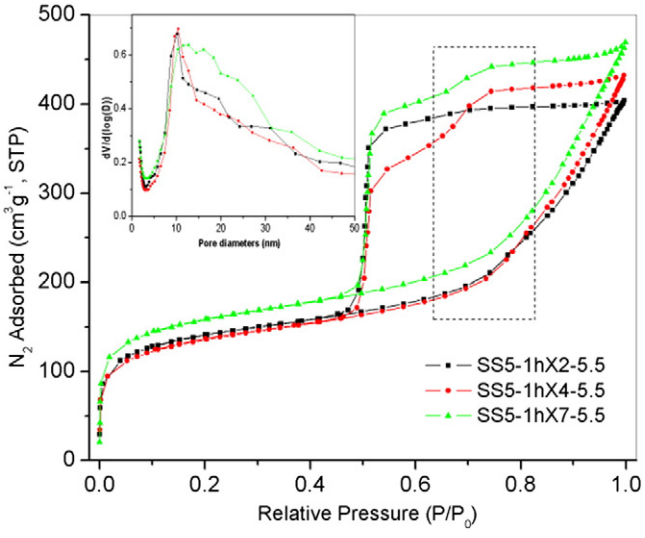

Fig. 4. N_2 sorption results of PCSA-II derived MS-MCFs with interval time of 1 h. The inset shows the corresponding PSDs calculated on the adsorption branches.

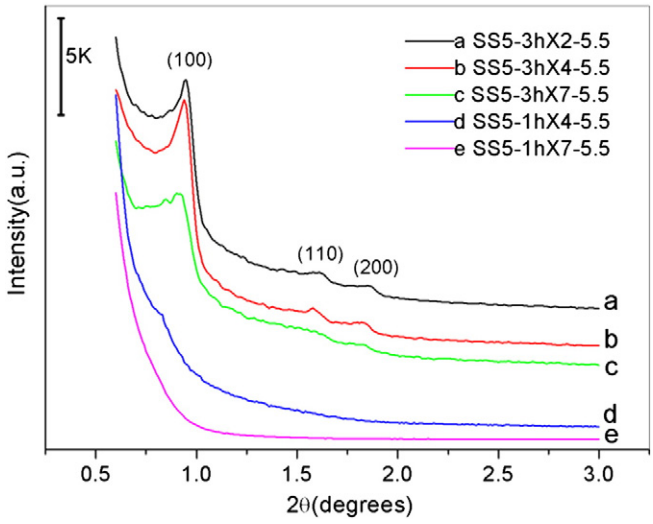

Fig. 5. Low-angle XRD patterns of PCSA-II route derived MS-MCFs. The reflections from the hexagonally ordered SBA-15 phases were labeled.

can only be attributed to the disturbed self-assembly process in the presence of hexane, leading to disordered mesostructures. In addition, two series of independent capillary condensation/evaporation steps also mean that two series of mesostructures are both accessible to the exteriors of the particles. Such MS-MCFs with mixed bimodal mesostructures of disordered cylindrical pores resemble those recently reported by Zhou et al., who employed a quaternary P123/cosurfactant/TMB/water templating system [30,31].

(2) For the MS-MCFs prepared with long interval time, i.e., 3 h, the isotherms of MS-MCFs prepared with different amounts of hexane, on the other hand, show some new characteristics (Fig. 6). The two-step feature of capillary condensation becomes even more evident. The larger capillary condensation steps at P/P_0 of 0.6–0.8 indicate the formation of significant proportions of mesostructures with cylindrical pores. Additionally, the tailing in the PSDs becomes less intense, suggesting the relatively diminished MCF structures templated from the hexane-swollen P123 micelles with long interval time (3 h). According to the low-angle XRD patterns, SS5-3hX*n*-5.5 ($n = 2, 4, 7$, Fig. 5, curve a–c) shows much more resolved low-angle XRD reflections than SS5-1hX4-5.5. At least three reflections can be identified, which can be indexed as (100), (110), and (200) reflections of a hexagonal symmetry lattice (p6mm), in line with the extensively reported SBA-15s [25,38]. The d_{100} peaks ($d_{100} = 9.3$ nm, and unit cell size, $a = 10.7$ nm) were not affected by the addition of different amounts of hexane. According to pore sizes calculated based on the N_2 sorption results (Fig. 6 and inset), wall thickness can be estimated to be 2.0–2.3 nm, consistent with previous reports [25]. Irrespective of the hexane dosages, the 1st mode mesopores are hexagonally ordered rather than disordered. This means that the hexane plays a limited role in the formation of these SBA-15 phases in the presence of progressively rigidified silicate/P123 interfaces in the PCSA-II route.

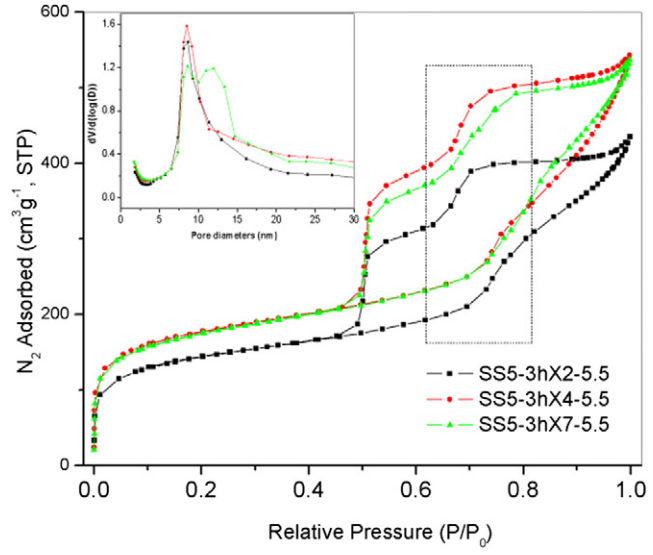

Fig. 6. N_2 sorption results of PCSA-II derived MS-MCFs with interval time of 3 h. The inset shows the corresponding PSDs calculated on the adsorption branches.

Therefore, in the PCSA-II route, the overall templating comprises two different templating mechanisms: one is the normal cooperative self-assembly process responsible for normal hexagonal SBA-15 type silicas (long-range ordering as shown by Fig. 5), and the other one is the microemulsion templating process (for the normal MCFs, though suppressed to a great extent). It is believed that, other than the influence of low solubility of hexane in the P123 micelles, the silicate species initially deposited on the P123 micelles 3 h after the 1st addition of SS can effectively restrict the penetration of hexane molecules into the hydrophobic P123 cores, while the interval time of 1 h (Fig. 4) is apparently not long enough to allow the silicate-P123 interface to sufficiently rigidify. When the interval times are extended from 1 h to 3 h, the interference of newly added swelling agent (i.e., hexane) with the P123 micelles becomes increasingly difficult. This can be seen from at least three aspects: (1) the formation of increased amounts of ordered SBA-15 phases. (2) The pore sizes of the first series of mesopores also become smaller (e.g., 10.4 nm for SS5-1hX4-5 and 8.5 nm for SS5-3hX4-5) with increased interval times, which can be explained by the less swelling effect of hexane on the P123 micelles (Table 1). (3) Such phenomena were also observed in the preparation of S-MCFs using TMB as pore swelling agent [ref. 26]. This again demonstrates the importance in tuning the silicate/P123 interface in the preparation of MS-MCFs via the PCSA-II route.

To clarify the arrangement of these ordered SBA-15 mesophases with respect to the coexisting MCFs structures, TEM measurements were carried out. As shown in Fig. 7 (more can be found in Fig. S2, Supplementary data), other than the disordered MCF structures, there are distinct areas of ordered SBA-15 phase with dimensions up to 200 nm embedded in an individual particle. The ordered mesopores

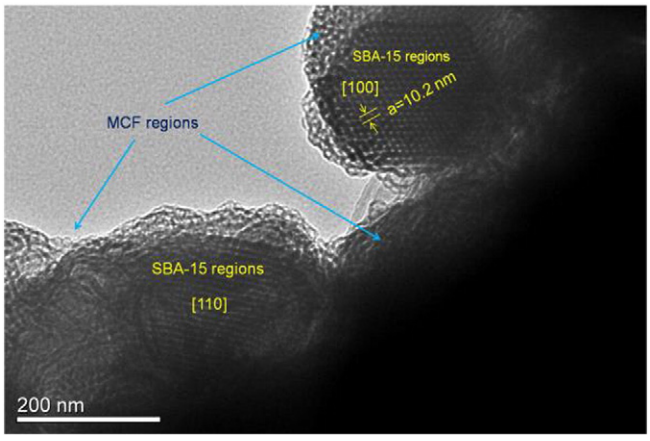

Fig. 7. TEM image of SS5-3hX7-5.5. Disordered MCF structures and ordered SBA-15 with different pore orientations were marked, as well as the interpore distance.

recorded along the [100] and channels along [110] directions were labeled in Fig. 7, respectively. The calculated interpore distance is about 10.2 nm. The TEM results are in good agreement with the XRD results (Fig. 6). Compared with previously reported MS-MCFs with SBA-15s phases prepared from TMB [26], the MS-MCFs prepared using hexane as pore swelling agent show two new characteristics: one is the significantly large (nearly doubled) SBA-15 domains, the other is that the proportions of the SBA-15 mesophase reported in this work (39–48%, Fig. 8) are ~50% larger than those in MCFs obtained from TMB (26–31%). Increases in the hexane only slightly decrease the proportions of the SBA-15 phases. Clearly, the PCSA-II route based on the SS as silica precursor and hexane as pore swelling agent can be used to produce MS-MCFs with high proportions of ordered SBA-15s mesophase, compared with those from TMB. This again should thank the low hexane solubility of hexane in P123 micelles, producing less swollen P123 micelles and therefore higher proportions of SBA-15 mesophase.

Currently, the preparation of bimodal mesoporous silicas mainly relies on either the employment of multiple templates [40–46], e.g., multiple surfactants, or specially designed synthetic procedures [47,48]. These measures might add to the complexity to the synthesis. By simply adjusting the order of adding the organic pore expanders (hexane in this work) to the synthesis mixture, MS-MCFs with bimodal pore size distributions can be facilely obtained, not to mention that the cheap sodium silicate was used as the inorganic precursor, rather than the most often employed tetraethoxysilane [49].

4. Conclusions

This work for the first time demonstrated that the hexane can serve as an interesting organic pore expander to swell the P123 micelles, allowing the preparation of modified mesocellular foams (MS-MCFs) with bimodal pores via a previously reported partitioned cooperative self-assembly (PCSA) process. Simple adjustments in the order of addition of hexane in the PCSA routes allow the preparation of two series of MS-MCFs: normal large-mesopore MCF structures modified with either disordered (PCSA-I route) or ordered SBA-15 (PCSA-II route) small-mesopore phases. In these syntheses, to tune the silicate/P123 interfaces is the key, which can be simply realized through adjusting the addition order of hexane relative to the addition of SS and the interval time in the PCSA routes, without resorting to any additives or complicated synthetic process. It is believed that this work opens new possibilities in tuning the mesostructures of MCFs and will further promote their application.

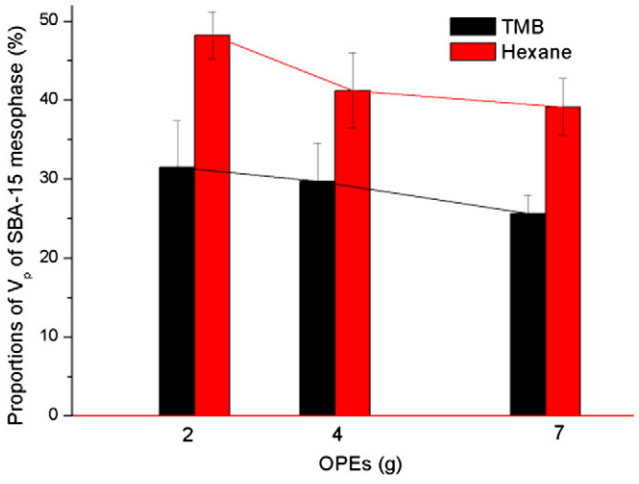

Fig. 8. The proportions of mesopores with pore size of 2–10 nm for MS-MCFs prepared using the same amounts (mass) of hexane and TMB as pore swelling agent and SS as silica precursor. The pore volumes were derived from the BDB method. And the data for TMB are based on the published results in ref. [26].

Acknowledgments

This work was supported by the National Natural Science Foundation of China (grant no. 21201030, 21471026, 51272039), the Fundamental Research Funds for the Central Universities (N141005001 and N100702001) and the Liaoning Province Innovation Funds (2014020030).

Appendix A. Supplementary data

Supplementary data to this article can be found online at http://dx.doi.org/10.1016/j.jnoncrysol.2015.06.007.

References

[1] P. Schmidt-Winkel, W.W. Lukens, D. Zhao, P. Yang, B.F. Chmelka, G.D. Stucky, Mesocellular siliceous foams with uniformly sized cells and windows, J. Am. Chem. Soc. 121 (1999) 254–255.
[2] P. Schmidt-Winkel, W.W. Lukens, P. Yang, D.I. Margolese, J.S. Lettow, J.Y. Ying, G.D. Stucky, Microemulsion templating of siliceous mesostructured cellular foams with well-defined ultralarge mesopores, Chem. Mater. 12 (2000) 686–696.
[3] P. Schmidt-Winkel, C.J. Glinka, G.D. Stucky, Microemulsion templates for mesoporous silica, Langmuir 16 (2000) 356–361.
[4] K. Szymańska, J. Bryjak, J. Mrowiec-Białoń, A.B. Jarzębski, Application and properties of siliceous mesostructured cellular foams as enzymes carriers to obtain efficient biocatalysts, Microporous Mesoporous Mater. 99 (2007) 167–175.
[5] X. Zhang, R. Guan, D. Wu, K. Chan, Enzyme immobilization on amino-functionalized mesostructured cellular foam surfaces, characterization and catalytic properties, J. Mol. Catal. B 33 (2005) 43–50.
[6] D. Gaffney, N.H. Abdallah, J.C. Cooney, F.R. Laffir, K.E. Cassimjee, P. Berglund, U. Hanefeld, E. Magner, Preparation and characterisation of a Ni^{2+}/Co^{2+}-cyclam modified mesoporous cellular foam for the specific immobilisation of His6-alanine racemase, J. Mol. Catal. B 109 (2014) 154–160.
[7] Z. Zhou, S. Zhu, D. Zhang, Grafting of thermo-responsive polymer inside mesoporous silica with large pore size using ATRP and investigation of its use in drug release, J. Mater. Chem. 17 (2007) 2428–2433.
[8] J. Zhao, Y. Wang, G. Luo, S. Zhu, Covalent immobilization of penicillin G acylase on aminopropyl-functionalized mesostructured cellular foams, Bioresour. Technol. 101 (2010) 7211–7217.
[9] L. Yang, Z. Gao, Y. Guo, W. Zhan, Y. Guo, Y. Wang, G. Lu, Paramagnetic epoxy-functionalized mesostructured cellular foams with an open pore system for immobilization of penicillin G acylase, Microporous Mesoporous Mater. 190 (2014) 17–25.
[10] X. Yan, L. Zhang, Y. Zhang, K. Qiao, Z. Yan, S. Komarneni, Amine-modified mesocellular silica foams for CO_2 capture, Chem. Eng. J. 168 (2011) 918–924.
[11] D.J.N. Subagyono, M. Marshall, G.P. Knowles, A.L. Chaffee, CO_2 adsorption by amine modified siliceous mesostructured cellular foam (MCF) in humidified gas, Microporous Mesoporous Mater. 186 (2014) 84–93.
[12] J. Ma, Q. Liu, D. Chen, Y. Zhou, S. Wen, Carbon dioxide adsorption using amine-functionalized mesocellular siliceous foams, J. Mater. Sci. 49 (2014) 7585–7596.
[13] P. Sharma, S.D. Park, K.T. Park, J.H. Park, C.Y. Jang, S.C. Nam, I.H. Baek, Mesoporous cellular foams supported $Fe_{2.0}SiW_{12}O_{40}$: synthesis, characterization and application to CO_2 sorption, Powder Technol. 233 (2013) 161–168.
[14] M. Trejda, J. Kujawa, M. Ziolek, J. Mrowiec-Białoń, Nb-containing mesoporous materials of MCF type—acidic and oxidative properties, Catal. Today 139 (2008) 196–201.
[15] Y.M. Liu, W.L. Feng, L.C. Wang, Y. Cao, W.L. Dai, H.Y. He, K.N. Fan, Chromium supported on mesocellular silica foam (MCF) for oxidative dehydrogenation of propane, Catal. Lett. 106 (2006) 145–152.
[16] Y. Su, Y.M. Liu, L.C. Wang, M. Chen, Y. Cao, W.L. Dai, H.Y. He, K.N. Fan, Tungsten-containing MCF silica as active and recyclable catalysts for liquid-phase oxidation of 1, 3-butanediol to 4-hydroxy-2-butanone, Appl. Catal. A 315 (2006) 91–100.
[17] Y.M. Liu, W.L. Feng, T.C. Li, H.Y. He, W.L. Dai, W. Huang, Y. Cao, K.N. Fan, Structure and catalytic properties of vanadium oxide supported on mesocellulous silica foams (MCF) for the oxidative dehydrogenation of propane to propylene, J. Catal. 239 (2006) 125–136.
[18] K. Stawicka, M. Trejda, M. Ziolek, The production of biofuels additives on sulphonated MCF materials modified with Nb and Ta—towards efficient solid catalysts of esterification, Appl. Catal. A 467 (2013) 325–334.
[19] A. Smuszkiewicz, J. López-Sanz, E. Pérez-Mayoral, E. Soriano, I. Sobczak, M. Ziolek, R.M. Martín-Aranda, A.J. López-Peinado, Amino-grafted mesoporous materials based on MCF structure involved in the quinoline synthesis. Mechanistic insights, J. Mol. Catal. A 378 (2013) 38–46.
[20] K. Stawicka, M. Trejda, M. Ziolek, New phospho-silicate and niobo-phospho-silicate MCF materials modified with MPTMS—structure, surface and catalytic properties, Microporous Mesoporous Mater. 181 (2013) 88–98.

[21] G. Wanka, H. Hoffmann, W. Ulbricht, Phase diagrams and aggregation behavior of poly (oxyethylene)-poly (oxypropylene)-poly (oxyethylene) triblock copolymers in aqueous solutions, Macromolecules 27 (1994) 4145–4159.
[22] J.M. Kim, Y. Sakamoto, Y.K. Hwang, Y.U. Kwon, O. Terasaki, S.E. Park, G.D. Stucky, Structural design of mesoporous silica by micelle-packing control using blends of amphiphilic block copolymers, J. Phys. Chem. B 106 (2002) 2552–2558.
[23] J.S. Lettow, Y.J. Han, P. Schmidt-Winkel, P. Yang, D. Zhao, G.D. Stucky, J.Y. Ying, Hexagonal to mesocellular foam phase transition in polymer-templated mesoporous silicas, Langmuir 16 (2000) 8291–8295.
[24] W. Wang, W. Shan, H. Ru, Facile preparation and new formation mechanism of plugged SBA-15 silicas based on cheap sodium silicate, J. Mater. Chem. 21 (2011) 17433–17440.
[25] W. Wang, W. Shan, H. Ru, N. Wu, A facile and versatile partitioned cooperative self-assembly process to prepare SBA-15s with larger mesopores, high microporosity and tunable particle sizes, J. Mater. Chem. 21 (2011) 12059–12067.
[26] W. Wang, W. Shan, X. Yue, H. Ru, Partitioned cooperative self-assembly process: taking the mesopore swelling strategy one step further for the preparation of mesocellular foams, J. Mater. Chem. 22 (2012) 3462–3470.
[27] R. Nagarajan, Solubilization of hydrocarbons and resulting aggregate shape transitions in aqueous solutions of Pluronic®(PEO–PPO–PEO) block copolymers, Colloids Surf. B 16 (1999) 55–72.
[28] M. Kruk, Access to ultralarge-pore ordered mesoporous materials through selection of surfactant/swelling-agent micellar templates, Acc. Chem. Res. 45 (2012) 1678–1687.
[29] H. Zhang, Y. Shen, Straight chain alkane-assisted synthesis of mesoporous silica, Mater. Lett. 75 (2012) 183–185.
[30] X. Zhou, A. Duan, Z. Zhao, Y. Gong, H. Wu, Y. Wei, G. Jiang, J. Liu, The influence of cosurfactants on the synthesis of hierarchically porous silica materials in a P123/cosurfactant/1,3,5-trimethylbenzene/water four-component microemulsion system, Mater. Lett. 133 (2014) 228–231.
[31] X. Zhou, A. Duan, Z. Zhao, Y. Gong, H. Wu, J. Li, Y. Wei, G. Jiang, J. Liu, Y. Zhang, Synthesis of hierarchically porous silicas with mesophase transformations in a four-component microemulsion-type system and the catalytic performance for dibenzothiophene hydrodesulfurization, J. Mater. Chem. A 2 (2014) 6823–6833.
[32] E.P. Barrett, L.G. Joyner, P.P. Halenda, The determination of pore volume and area distributions in porous substances. I. computations from nitrogen isotherms, J. Am. Chem. Soc. 73 (1951) 373–380.
[33] J. Broekhoff, J. De Boer, Studies on pore systems in catalysts: IX. Calculation of pore distributions from the adsorption branch of nitrogen sorption isotherms in the case of open cylindrical pores A. Fundamental equations, J. Catal. 9 (1967) 8–14.
[34] J. Broekhoff, J. De Boer, Studies on pore systems in catalysts: XI. Pore distribution calculations from the adsorption branch of a nitrogen adsorption isotherm in the case of "ink-bottle" type pores, J. Catal. 10 (1968) 153–165.
[35] J. Broekhoff, J. De Boer, Studies on pore systems in catalysts: XII. Pore distributions from the desorption branch of a nitrogen sorption isotherm in the case of cylindrical pores A. An analysis of the capillary evaporation process, J. Catal. 10 (1968) 368–376.
[36] J.R. Matos, M. Kruk, M. Jaroniec, L. Zhao, T. Kamiyama, O. Terasaki, T.J. Pinnavaia, Y. Liu, Ordered mesoporous silica with large cage-like pores: structural identification and pore connectivity design by controlling the synthesis temperature and time, J. Am. Chem. Soc. 125 (2003) 821–829.
[37] M. Kruk, V. Antochshuk, J.R. Matos, L.P. Mercuri, M. Jaroniec, Determination and tailoring the pore entrance size in ordered silicas with cage-like mesoporous structures, J. Am. Chem. Soc. 124 (2002) 768–769.
[38] D. Zhao, J. Feng, Q. Huo, N. Melosh, G.H. Frederickson, B.F. Chmelka, G.D. Stucky, Triblock copolymer syntheses of mesoporous silica with periodic 50 to 300 angstrom pores, Science 279 (1998) 548–552.
[39] D. Zhao, Q. Huo, J. Feng, B.F. Chmelka, G.D. Stucky, Nonionic triblock and star diblock copolymer and oligomeric surfactant syntheses of highly ordered, hydrothermally stable, mesoporous silica structures, J. Am. Chem. Soc. 120 (1998) 6024–6036.
[40] M. Groenewolt, M. Antonietti, S. Polarz, Mixed micellar phases of nonmiscible surfactants: mesoporous silica with bimodal pore size distribution via the nanocasting process, Langmuir 20 (2004) 7811–7819.
[41] A. May, M.J. Stébé, J.M. Gutiérrez, J.L. Blin, Coexistence of two kinds of fluorinated hydrogenated micelles as building blocks for the design of bimodal mesoporous silica with two ordered mesopore networks, Langmuir 27 (2011) 14000–14004.
[42] R. Xing, H. Lehmler, B.L. Knutson, S.E. Rankin, Synthesis and tuning of bimodal mesoporous silica by combined hydrocarbon/fluorocarbon surfactant templating, Langmuir 25 (2009) 6486–6492.
[43] J. Sun, Z. Shan, T. Maschmeyer, J.A. Moulijn, M.O. Coppens, Synthesis of tailored bimodal mesoporous materials with independent control of the dual pore size distribution, Chem. Commun. 24 (2001) 2670–2671.
[44] K. Suzuki, K. Ikari, H. Imai, Synthesis of silica nanoparticles having a well-ordered mesostructure using a double surfactant system, J. Am. Chem. Soc. 126 (2004) 462–463.
[45] L. Chen, W. Zhang, J. Xu, D.A. Tanner, M.A. Morris, Mesopore constrictions derived from the substitutionally co-packed SBA-15, Microporous Mesoporous Mater. 129 (2010) 179–188.
[46] D. Niu, Z. Ma, Y. Li, J. Shi, Synthesis core–shell structured dual-mesoporous silica spheres with tunable pore size and controllable shell thickness, J. Am. Chem. Soc. 132 (2010) 15144–15147.
[47] Z.Y. Yuan, J.L. Blin, B.L. Su, Design of bimodal mesoporous silicas with interconnected pore systems by ammonia post-hydrothermal treatment in the mild-temperature range, Chem. Commun. 5 (2002) 504–505.
[48] N. Li, J. Wang, H. Zhou, P. Sun, T. Chen, Synthesis of single-crystal-like, hierarchically nanoporous silica and periodic mesoporous organosilica, using polyelectrolyte-surfactant mesomorphous complexes as a template, Chem. Mater. 23 (2011) 4241–4249.
[49] W. Wang, H. Qi, H.B. Long, X. Wang, H.Q. Ru, A simple ternary non-ionic templating system for preparation of complex hierarchically meso-mesoporous silicas with 3D interconnected large mesopores, J. Mater. Chem. A 2 (2014) 5363–5370.